26 May 2010, 11:30 am - 12:00 pm

Liquefaction-Induced Movements of Buildings with Shallow Foundations

Jonathan D. Bray
University of California Berkeley, Berkeley, CA

Shideh Dashti
University of California Berkeley, Berkeley, CA


Fifth International Conference on
Recent Advances in Geotechnical Earthquake Engineering and Soil Dynamics
and Symposium in Honor of Professor I.M. Idriss
May 24-29, 2010 • San Diego, California

LIQUEFACTION-INDUCED MOVEMENTS OF BUILDINGS WITH SHALLOW FOUNDATIONS

Jonathan D. Bray
University of California, Berkeley
Berkeley, CA 94720-1710

Shideh Dashti
University of California, Berkeley
Berkeley, CA 94720-1710

ABSTRACT

Seismically induced settlement of buildings with shallow foundations on liquefiable soils has resulted in significant damage in recent earthquakes. In Adapazari, Turkey multi-story buildings punched into, tilted excessively, and slid laterally on softened ground. The state-of-the-practice still largely involves estimating building settlement using empirical procedures developed to calculate post-liquefaction consolidation settlement in the free-field. This approach cannot possibly capture shear-induced and localized volumetric-induced deformations in the soil underneath shallow mat foundations. Geotechnical centrifuge experiments were performed recently to identify the dominant mechanisms involved in liquefaction-induced building settlement. The centrifuge tests revealed that considerable building settlement occurs during earthquake strong shaking. Volumetric strains due to localized drainage in response to high transient hydraulic gradients and deviatoric strains due to shaking-induced ratcheting of the buildings into the softened soil are important effects that are currently not captured in current procedures. The relative importance of each mechanism depends on the characteristics of the earthquake motion, liquefiable soil, and building. The initiation, rate, and amount of liquefaction-induced building settlement depend greatly on the shaking intensity rate (*SIR*) of the ground motion. Preliminary recommendations for estimating liquefaction-induced movements of buildings with shallow foundations are made. However, additional work is warranted.

INTRODUCTION

The state-of-the-practice for estimating liquefaction-induced building settlement relies heavily on empirical procedures developed to estimate post-liquefaction consolidation settlement in the free-field, without the effects of structures (e.g., Tokimatsu and Seed 1987; Ishihara and Yoshimine 1992). Estimating building settlement based on free-field, post-liquefaction, reconsolidation volumetric strains neglects the importance of other mechanisms that could damage the structure and its surrounding utilities. Effective mitigation of the soil liquefaction hazard requires a thorough understanding of the potential consequences of liquefaction and the building performance objectives. The consequences of liquefaction, in turn, depend on site conditions, earthquake loading characteristics, and the structure. Hence, a rational design of site-specific liquefaction mitigation techniques requires a better understanding of the influence of these factors on the consequences of liquefaction.

BUILDING SETTLEMENT IN ADAPAZRI, TURKEY

Observations after the 1999 Kocaeli earthquake

A large percentage of structures in Adapazari, Turkey collapsed or were heavily damaged due to strong ground shaking during the August 17, 1999 Kocaeli (M_w = 7.5) earthquake. Many structures were also damaged by ground failure due to liquefaction/cyclic softening of shallow silt and sand deposits. Ground failure was indicated by punching of buildings into the ground, excessive building tilt with ground heave, and lateral translation of buildings over softened ground. The occurrence of structural damage was found to be related to the occurrence of ground failure (Sancio et al. 2002, Bray et al. 2004, Sancio et al. 2004).

Most of the Adapazari is located over deep sediments (Sancio et al. 2002) in what is a former Pliocene-Pleistocene lake. The lake sediments are overlain by Pleistocene and early-Holocene alluvium transported from the mountains north and south of the basin. The shallow soils (depth < 10 m) are recent Holocene deposits laid down by the Sakarya and Çark rivers, which frequently flooded the area until flood control dams were built recently. Sands accumulated along bends of the meandering rivers, and the rivers flooded periodically leaving behind predominantly nonplastic silts, silty sands, and clays throughout the city.

Buildings are primarily 3 to 6 story reinforced concrete buildings designed with a beam-column system (Sancio et al. 2004). Interior walls are built with hollow clay bricks covered

with stucco, and exterior walls generally consist of lighter, porous, solid blocks to provide thermal insulation. The building roofs are inclined slightly and covered with clay tiles. Older buildings of 1 to 2 stories that were built with timber and clay bricks are also found, but they are less prevalent.

The reinforced concrete building foundations in Adapazari are unusually robust. They typically consist of a 30 to 40 cm thick reinforced concrete mat that is stiffened with 30 cm wide and 100 cm to 120 cm deep reinforced concrete grade beams that are typically spaced between 4 m and 6 m in both directions. The open cells between adjacent grade beams are filled with compacted soil and then covered with a thin concrete floor slab. This foundation system is essentially a very stiff and strong mat that is about 1.5 m thick. As a result of ground failure, many structures moved excessively without significant structural damage. The nearly rigid foundations allowed the building to respond more as a rigid body (if the overlying structural system does not fail) while it undergoes significant differential downward movement, tilt, or lateral translation.

Many buildings in Adapazari sunk into the ground, often without noticeable tilt as is shown for the case of Fig. 1. At times, heave of the surrounding ground was observed. Some buildings experienced non-uniform vertical deformation, causing the building to be condemned albeit devoid of structural damage as for the example shown in Fig. 2. Toppling of buildings was typically observed in laterally unconstrained slender buildings, i.e. large ratio of building height (H) to its width (B). Some buildings translated laterally over liquefied soil directly beneath their foundation, as shown in the example Fig. 3. The structure displaced approximately 31 cm away from the previously adjacent sidewalk.

Fig. 1 First floor of a multi-story building that has punched approximately 30 cm into the ground.

Fig. 2. Vertical building settlement with significant tilt.

Fig. 3. Lateral translation of building on softened ground.

Findings in Adapazari

In downtown Adapazari, most of the buildings have foundations that are 5 m to 20 m wide. Buildings in this area with foundation widths in this range typically experienced relative vertical displacement between 0 cm and 30 cm. The average measured relative vertical displacement (Δ) divided by the width of the building (B) is plotted in Fig. 4 as a function of the height of the building (H) divided by the width of the building (B) for structures founded at sites containing shallow liquefiable soils. The height of the building divided by the width (H/B) is known as the aspect ratio, but it is also related to the contact pressure (q). As described previously, excessive building tilt or even toppling was sometimes observed in laterally unconstrained buildings with high aspect ratios. Buildings that experienced excessive tilt or toppling have been excluded from Fig. 6.

Examining Fig. 4, the amount of vertical displacement of the building relative to the surrounding ground is found to be roughly proportional to the aspect ratio of the building (H/B),

which is relatively equivalent to the applied contact pressure (q). All else being equal, buildings of higher contact pressure (and also higher aspect ratio) experienced more vertical displacement. Taller, heavier buildings experienced greater vertical movement than the smaller, lighter buildings.

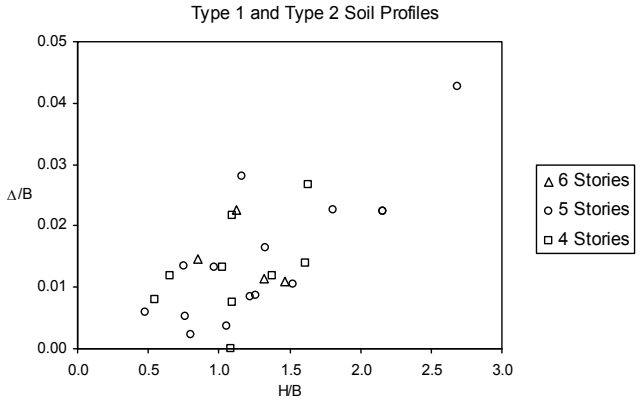

Fig. 4. Relationship between building settlement (Δ) and the building height (H) normalized by the foundation width (B) [from Sancio et al. 2004].

Figure 5 depicts two common modes of building performance observed in Adapazari after the Kocaeli earthquake. A stout building with a large mat foundation, where its width is much greater than the thickness of the underlying liquefiable silt deposit, is shown on the left and a slender building with a narrow foundation width is shown on the right in Fig. 5.

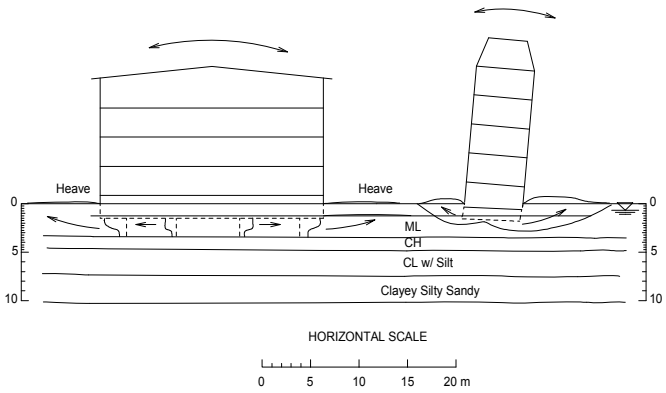

Fig. 5. Modes of failure of stout and slender buildings in Adapazari [from Sancio et al. 2004].

Based on the interpretation of the results of the in situ tests (Bray et al. 2004), the shallow silt deposit (ML) shown in Fig. 5 was identified as the critical layer under most of the buildings studied in Adapazari. The liquefiable silt has a low plasticity index (PI < 12) and high water content to liquid limit ratio (w_c/LL > 0.85) (Bray and Sancio 2006). Deeper deposits (i.e., 5 m < depth < 10 m) of silt and sand were often too dense to have liquefied. Deeper silt strata that were potentially liquefiable exhibited significantly greater cyclic strength than the shallow silt (Bray et al. 2004). Although at some sites the deeper layers might have contributed to the overall building performance, this contribution will be neglected for the sake of this discussion, because it appears that in many cases the response of the upper silt dominated the building response. It can therefore be assumed, without considerable error, that only the silt layer (ML) shown in Fig. 5 lost significant strength during the earthquake.

The earthquake-induced shear stresses imposed on the soil elements under the stout building caused an immediate generation of positive excess pore water pressure and subsequent loss of strength and stiffness. Additionally, the soil in the free-field has also developed significant pore water pressure and perhaps is undergoing liquefaction. Under these conditions, it can be surmised that the soil under the stout building can no longer withstand the weight of the structure, and thus, it is squeezed out laterally. As the soil is sheared it dilates eventually and recovers its shear strength so it can once again resist the weight of the structure. Thus, in addition to this "partial loss of bearing" phenomenon, cyclic loading of the soil through inertial interaction of the heavy building is required to work the building repeatedly into the softened soil.

Given that the failure is shallow, the initial squeezing can cause some heave at the surface as was observed at some of these sites. However, the number of sites where appreciably heave was observed was limited, and typically noticeably heave was observed at sites where buildings tilted excessively (Bray and Stewart 2000). Thus, for buildings to punch into the surrounding ground without noticeably heave, as shown in Fig. 1, significant volumetric strain must have occurred during strong shaking. Localized drainage of soils that developed high excess pore water pressures and thus produced steep hydraulic gradients must have occurred.

The performance of the slender building in Fig. 5 is more representative of a typical bearing-type failure where the soil deforms along a failure surface. Again, the earthquake shaking generates of positive pore water pressures in the liquefiable soil which causes it to temporarily lose strength. Additionally, horizontal shaking causes the building to apply a dynamic overturning moment at the foundation level. The magnitude of the overturning moment and thus the eccentricity is a function of the seismic response of the building and the height, width, and weight of the building.

If the mat foundation is narrow, the effect of the eccentric load is greater because it causes stress concentrations over a smaller area of the mat foundation. When this stress approaches or exceeds the seismic bearing capacity of the soil (i.e., considering the reduction of strength due to excess pore water pressure), the building begins to tilt. As tilting is initiated, the area over which the stresses are applied is reduced, thus the magnitude of the stress increases. Under these conditions, a progressive failure is possible. Continuing tilt will cause toppling unless the bearing capacity of the soil increases sufficiently due to dilation of the soil or due to an

increase of effective stress due to dissipation of excess pore water pressure, or cessation of shaking which causes the cyclic overturning moment to reduce significantly.

Summary of Observations in Adapazari

Buildings in Adapazari were essentially stiff structures (until they underwent brittle failure) founded on very stiff and strong thick mat foundations. Although there were countless examples of poorly designed or constructed structures that failed due to strong shaking, many of these buildings were damaged by ground failure. Ground failure largely resulted from cyclic softening or liquefaction of shallow low plasticity silty soils in the upper few meters of the soil profile. Measured vertical displacements of the buildings relative to the surrounding ground were larger than what could be explained by post-liquefaction reconsolidation settlement. Moreover, seismically induced ground settlements in the free-field were significantly less than seismically induced building settlements.

Shear-induced deformation and localized volumetric strain under the building foundations must have contributed to the relatively large building settlements. Building settlements were significantly greater for taller, heavier buildings than for shorter, lighter buildings. Tall buildings with relatively narrow foundation widths were prone to tilt excessively or topple. Although much can be learned from the building movement case histories documented in Adapazari there are significant uncertainties such as good characterization of the earthquake shaking. Thus, additional investigations of these phenomena are warranted.

PREVIOUS STUDIES

Previous empirical studies have found that earthquake-induced vertical displacements of foundations on granular soils are related to the width and contact pressure of the foundation and the thickness of the liquefied soil layer, among other factors (e.g., Yoshimi and Tokimatsu 1977; Liu 1995; Shahien 1998). Fig. 6 shows the observed trends in building settlement based on the available case histories (Liu and Dobry 1997). This figure shows that liquefaction-induced foundation settlement is inversely proportional to the foundation width. In line with these observations, Ishii and Tokimatsu (1988) proposed that if the width of the foundation is sufficiently larger than the thickness of the liquefiable layer, the settlement of the structure is nearly equal to that in the free-field. Conversely, if the ratio of the width of the foundation to the thickness of the liquefied layer is less than about 3, then structures appeared to settle more than the volumetric strains observed in the free-field.

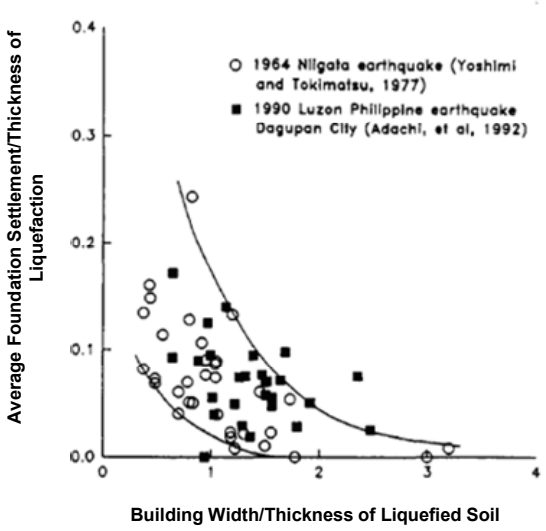

Fig. 6. Normalized foundation settlement versus normalized foundation width based on the available case histories [from Liu and Dobry 1997].

Several researchers have used small-scale shaking table and centrifuge tests to study the seismic performance of rigid, shallow model foundations situated atop deep, uniform deposits of saturated, loose-to-medium dense, clean sand (e.g., Yoshimi and Tokimatsu 1977; Liu and Dobry 1997; Hausler 2002). Most of the building settlements were shown to occur during strong shaking, with a smaller contribution resulting from post-shaking soil reconsolidation due to excess pore water dissipation. Foundations settled in an approximately linear manner with time during shaking and commonly settled more than the free-field soil. As a result, building settlements were recognized to be strongly influenced by the structure's inertial forces (Liu and Dobry 1997). The effects of key testing parameters on the building's seismic performance, however, were not well characterized.

Increasing the relative density (D_r) and the over-consolidation ratio (OCR) of the liquefiable sand layer was shown to decrease the rate of excess pore water pressure generation and decrease seismically induced settlements (e.g., Adalier and Elgamal 2005). The degree of excess pore water pressure generation and soil softening was found to depend significantly on the confining pressure and foundation-induced static and dynamic shear stresses. No clear pattern was identified for the direction of flow and the degree of soil softening under and around structures as a function of various input parameters. Partial drainage was shown to occur simultaneously with excess pore pressure generation, as fast pore water pressure redistribution took place in a three-dimensional (3-D) pattern in response to transient hydraulic gradients (e.g., Liu and Dobry 1997). However, the influence of drainage on building settlements during earthquake strong shaking has not been defined clearly.

The mechanism of void redistribution within a submerged layer of liquefied sand beneath a less pervious layer and the formation of water inter-layers (an extreme case of void redistribution) under level ground conditions have been investigated in several physical model studies (e.g., Elgamal et al. 1989; Dobry and Liu 1992; Kokusho 1999). Under mildly sloping ground conditions, shear strain localization occurred at the interface between the loose sand layer and an overlying low-hydraulic conductivity layer in numerous centrifuge models. The intensity of shear strain localization depended on initial soil properties, slope-induced static shear stresses, and shaking characteristics (e.g., Fiegel and Kutter 1994; Kulasingam et al. 2004). However, the dynamic response of shallow foundations founded on a layered soil deposit of varying hydraulic conductivities that includes a liquefiable soil stratum has not been studied adequately.

There are presently no well-calibrated design procedures for estimating the combined and complex effects of deviatoric and volumetric settlements due to cyclic softening under the static and dynamic loads of structures. This is in contrast with those procedures available for evaluating liquefaction triggering and post-liquefaction re-consolidation settlements in the free-field (e.g., Tokimatsu and Seed 1987; Ishihara and Yoshimine 1992).

The state-of-the-practice for estimating liquefaction-induced building settlement relies heavily on empirical procedures developed to estimate post-liquefaction consolidation settlement in the free-field (i.e., without the influence of structures). Practicing engineers often use a combination of the available empirical methods (e.g., Tokimatsu and Seed 1987; Ishihara and Yoshimine 1992) and Fig. 6, which is based on the available case histories that all have relatively thick layers of liquefiable sand, with the application of significant engineering judgment and experience to assess the likely deformations and their impact on structures and other engineered facilities. There is a relative lack of understanding of the underlying mechanisms of liquefaction-induced building movements. Hence, there is a lack of reliable and well-calibrated analysis tools for use in engineering practice.

The lack of understanding of the underlying mechanisms often leads engineers to erroneous conclusions. In contrast to the observations of building performance at sites with thick liquefiable soil layers that had been made following previous earthquakes, many of the structures in Adapazari, Turkey that were damaged during the 1999 Kocaeli Earthquake were affected by the liquefaction of relatively thin layers of loose, saturated soils. The significant levels of building settlement commonly observed in Adapazari cannot be estimated using available empirical relations, because the thickness of the liquefiable soil layer in Adapazari was commonly only a few meters thick.

Additionally, the inertial loading of structures appeared to be largely detrimental in Adapazari during the 1999 Kocaeli Earthquake, because ground failure was systematically observed near structures and less so away from the buildings (Sancio et al. 2002). The most common mechanism of building settlement in Adapazari during this earthquake was believed to be the rapid spreading of the soil directly under the building outward due to a temporary loss of bearing capacity and soil-structure-interaction (SSI) ratcheting of buildings into the softened ground. Building's contact pressure and height/width (*H/B*) ratio were found to greatly influence the amount of building settlement and tilt, respectively (Sancio et al. 2004). Therefore, the width of the foundation and the thickness of the liquefiable layer were shown to be insufficient for predicting building response on softened ground.

GEOTECHNICAL CENTRIFUGE TESTING PROGRAM

Without a sufficient number of well-documented case histories, carefully performed physical model tests offer a means for better understanding the performance of buildings founded on liquefiable soils. Accordingly, a series of centrifuge experiments were performed by Dashti (2009) to generate model "case studies" of building response on liquefied ground. The soil response in the free-field was compared to that observed in the ground surrounding the structures, and the dominant mechanisms of settlement at different locations were identified.

Four geotechnical centrifuge experiments were performed to gain insight into the seismic performance of buildings with rigid mat foundations on a relatively thin deposit of liquefiable, clean sand. These experiments are described in more detail in Dashti (2009), Dashti et al. (2010a), and Dashti et al. (2010b). Table 1 provides a summary of the centrifuge testing program. Centrifuge experiments were conducted at a spin acceleration of 55 g. All units in this paper are provided in prototype scale. The thickness (H_L) and the relative density (D_r) of the liquefiable layer and the structural properties of the models were varied in the first three experiments to identify key parameters affecting soil and structural response and the primary mechanisms involved in liquefaction-induced building settlement. The fourth experiment (T3-50) examined the influence of ground motion characteristics, the relative importance of key settlement mechanisms, and the effectiveness of two mitigation strategies.

Figure 7 presents the plan view and cross section of the model used in experiment T3-30. Over 120 measurement devices (i.e., accelerometers, pressure transducers, and LVDTs) were employed in each experiment. The three tests referred to as T3-30, T3-50-SILT, and T3-50 included a liquefiable soil layer with a prototype thickness (H_L) of 3 m and nominal relative densities (D_r) of 30%, 50%, and 50%, respectively. In T3-50-SILT, the 2-m thick Monterey Sand placed on top of liquefiable Nevada Sand in the other experiments was replaced by a 0.8 m thick layer of silica flour underlying a 1.2 m thick layer of Monterey Sand. Test T6-30, with H_L = 6 m and D_r = 30%, provided information regarding the effects of the liquefiable layer thickness.

The lower deposit of uniform, fine Nevada Sand (D_{50} = 0.14 mm, $C_u \approx 2.0$, $e_{min} \approx 0.51$, $e_{max} \approx 0.78$) was dry pluviated to attain $D_r \approx 90\%$. The same Nevada Sand with an initial nominal D_r of either 30% or 50% was then placed by dry pluviation. This 3 m or 6 m thick layer of loose or medium dense Nevada Sand was the primary liquefiable material in these experiments. The hydraulic conductivities of Nevada Sand and silica flour are approximately 5 x 10^{-2} and 3 x 10^{-5} cm/s, respectively, when water is used as the pore fluid (Fiegel and Kutter 1994). A solution of hydroxypropyl methylcellulose in water was used as the pore fluid in these experiments with a viscosity of approximately 22(±2) times that of water (Stewart et al. 1998). The model was placed under vacuum and then flooded with CO_2 before saturation with the pore fluid. The phreatic surface was maintained approximately 1.1 m below the ground surface.

Table 1. Centrifuge Model Tests of Dashti (2009)

Test	H_L/D_r	Structural Models	Ground Motion Characteristics			
			Record	*PGA* (g)	$D_{5\text{-}95}$ (s)	I_a (m/s)
T6-30	6 m / 30%	Elastic building on mat: W x L x H A: 6 x 9 x 5 m B: 12 x 18 x 5 m C: 6 x 9 x 9.2 m	Mod. P.I. 1995 Kobe	0.15	8	0.4
T3-30	3 m / 30%					
T3-50-SILT	3 m / 50%; with silt layer		Large P.I. Kobe	0.55	9	4.5
T3-50	3 m / 50%		Mod. P.I. Kobe	0.15	8	0.3
			TCU078 1999 Chi-Chi	0.13	28	0.6
			Large P.I. Kobe	0.38	11	2.7

Notes: 1. H_L = Thickness of liquefiable soil layer
2. D_r = Relative density of liquefiable soil layer
3. *PGA* = Peak ground acceleration
4. $D_{5\text{-}95}$ = Significant duration
5. I_a = Arias intensity
6. *P.I.* = Port Island down-hole record

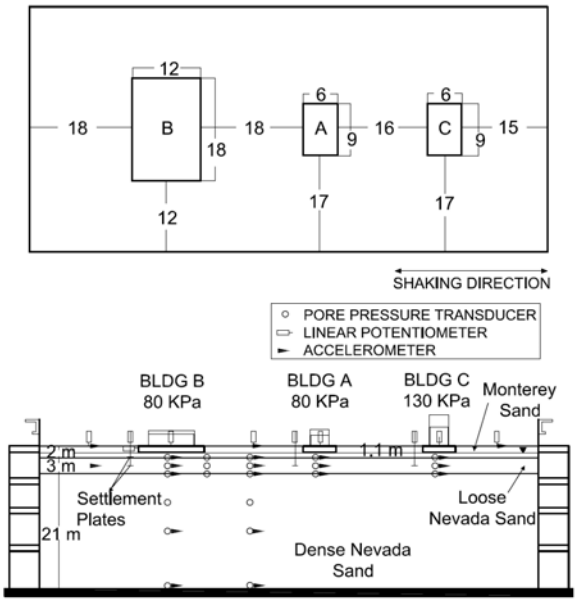

Fig. 7. Centrifuge model in experiment T3-30. Dimensions are in meters in prototype scale (Dashti et al. 2010a).

All structural models were single-degree-of-freedom, elastic, flexible structures made of steel and aluminum placed on a 1 m-thick, rigid mat foundation. The baseline structure (A) represented a 2-story, stout building with a contact pressure of 80 kPa; a second structure (B) had an increased footing contact area but the same contact pressure; and a third structure (C) represented a taller 4-story building with increased bearing pressure of 130 kPa. The fixed-base natural period of the structures ranged from 0.2 to 0.3 sec. Three structures similar to Structure A were used in T3-50 with different liquefaction remediation techniques.

A series of realistic earthquake motions (Table 1) were applied to the base of the model consecutively in each experiment. Sufficient time between shakes was allowed to ensure full dissipation of excess pore pressures. Figure 8 shows displacement- and acceleration-time histories of two different ground motions that were used. The input motions included a sequence of scaled versions of the north-south, fault-normal component of the 1995 Kobe Port Island motion that was recorded at a depth of 80 m and a modified version of the fault-normal component of the ground motion recorded at the free-field TCU078 station during the 1999 Chi-Chi Taiwan Earthquake with a peak base acceleration of 0.13 g.

DISPLACEMENT MECHANISMS

Case studies and physical model tests indicate that seismically induced cyclic pore water pressure generation and liquefaction (i.e., $u_e \cong \sigma'_{vo}$, where u_e is the excess pore water pressure and σ'_{vo} is the initial overburden effective stress) may produce or intensify several mechanisms of settlement, which can damage structures as well as the surrounding utilities. Deformations

resulting from earthquake loading may be categorized as either volumetric- or deviatoric-induced deformations. Based on the work of Dashti (2009), Dashti et al. (2010a), and Dasthi et al. (2010b), the primary settlement mechanisms involved in liquefaction-induced building movements are described. The volumetric and deviatoric strains that develop at any location are a function of the interactions between free-field and structure-induced cyclic demands as well as static shear stresses imposed by the foundation and are conceptually divided into separate categories for clarity.

The primary volumetric-induced settlement mechanisms are:

- Localized volumetric strains during partially drained cyclic loading controlled by 3-D transient hydraulic gradients ($\varepsilon_{p\text{-}DR}$) (Fig. 9a);
- Settlements due to sedimentation or solidification after liquefaction or soil structure break-down ($\varepsilon_{p\text{-}SED}$); and
- Consolidation-induced volumetric strains as excess pore water pressures dissipate and the soil's effective stress increases ($\varepsilon_{p\text{-}CON}$);

Deviatoric (shear-induced) soil deformations near a structure can be critical, particularly at intense shaking levels. They depend on static driving shear stresses caused by the foundation bearing loads ($\alpha = \tau_{static}/\sigma'_{vo}$) and the SSI-induced cyclic loads, as well as the soil properties. The primary deviatoric-induced settlement mechanisms are:

- Partial bearing failure under the static load of structures due to strength loss in the foundation soil resulting in punching settlements or tilting of the structure ($\varepsilon_{q\text{-}BC}$) (Fig 9b); and
- Cumulative ratcheting foundation settlements due to SSI-induced cyclic loading near the edges of the foundation ($\varepsilon_{q\text{-}SSI}$) (Fig. 9c).

The effects of each of these settlement mechanisms and their relative contribution to the total building movement are expected to be a function of the soil and structural properties and the ground motion characteristics.

SETTLEMENT OF GROUND AWAY FROM BUILDINGS

Free-field acceleration response spectra recorded during the moderate Port Island event in experiments T3-30, T3-50-SILT, and T3-50 are compared in Fig. 10 (all models had a liquefiable layer thickness of 3 m and similar loading histories up to this point). The higher relative density of the liquefiable layer in T3-50-SILT and T3-50 ($D_r \approx 50\%$) led to larger dilation cycles and less soil damping relative to T3-30 ($D_r \approx 30\%$), and hence produced larger spectral accelerations. As expected, the surface ground shaking increased as the sand's relative density and stiffness increased, intensifying the dynamic loads experienced by the structure.

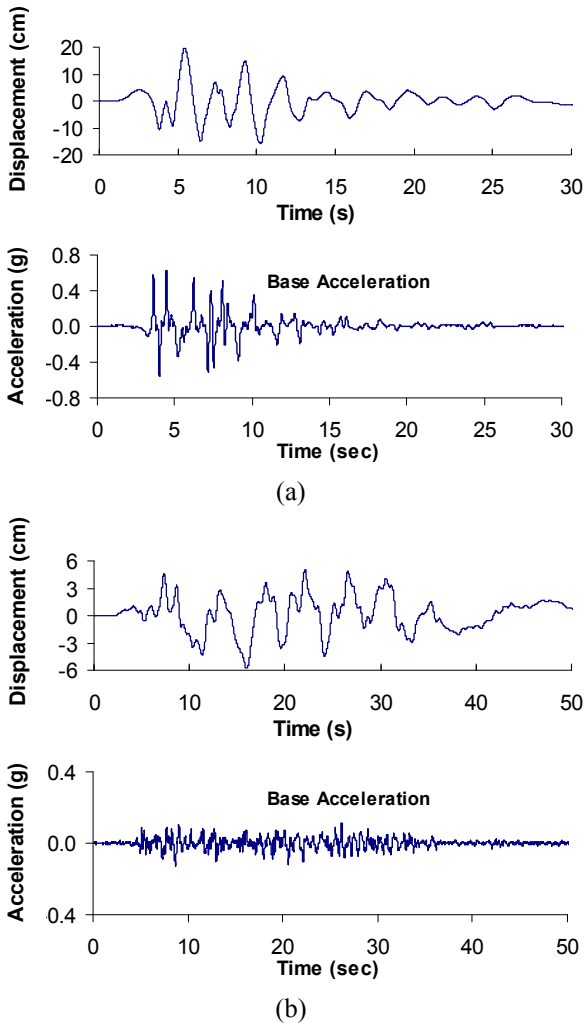

Fig. 8. Input base displacement- and acceleration-time histories: (a) large Port Island motion in experiment T6-30; and (b) Chi-Chi TCU078 motion in experiment T3-50.

Figure 11 presents representative excess pore water pressure-time histories and total head isochrones measured in the free-field during the moderate Port Island event in T3-50. The looser layer of Nevada Sand liquefied ($u_e \cong \sigma'_{vo}$) after about 2-3 sec of strong shaking and large vertical, upward transient hydraulic gradients were created and maintained during strong shaking in the free-field. These hydraulic gradients led to a significant flow potential from the lower deposit of Nevada Sand upward after a few seconds of strong shaking.

Representative excess pore water pressure- and settlement-time histories recorded in the free-field during the moderate Port Island event in T3-30, T3-50-SILT, and T3-50 are shown in Fig. 12. The input base acceleration time-history recorded during T3-50 is also shown. Positive displacement in the upper plot indicates settlement. Free-field settlements occurred during strong shaking, which suggested that partial drainage occurred during strong shaking. The assumption of a globally undrained loading was not valid in these experiments.

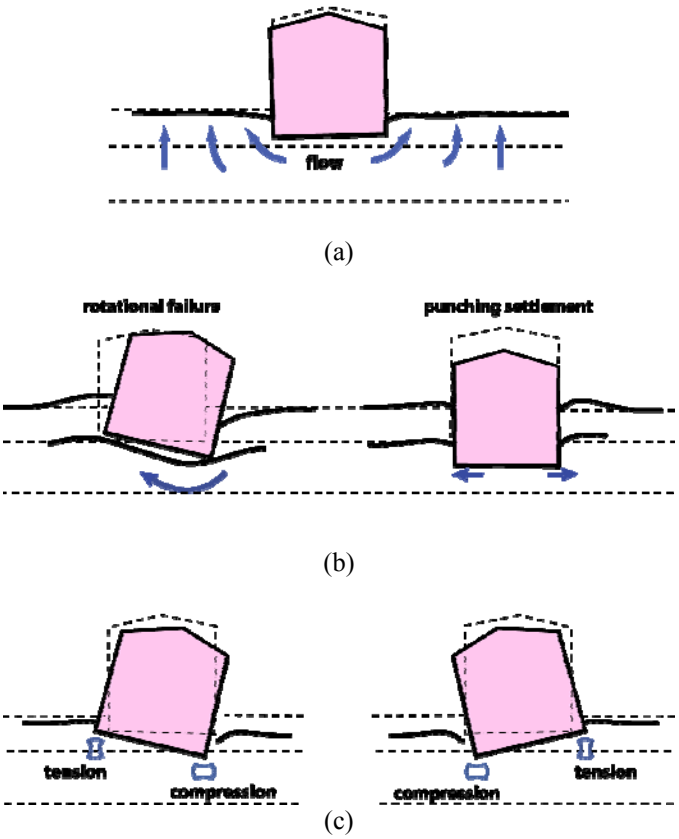

Fig. 9. Liquefaction-induced displacement mechanisms: (a) volumetric strains caused by water flow in response to transient gradients; (b) partial bearing capacity failure due to soil softening; and (c) SSI-induced building ratcheting during earthquake loading.

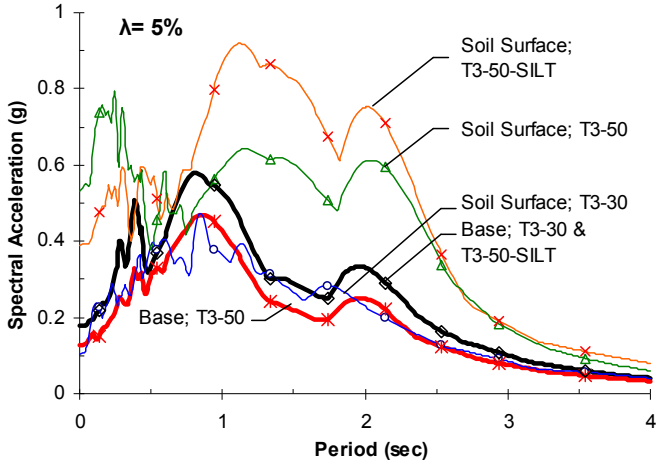

Fig.10. Horizontal acceleration response spectra (5% damped) recorded on the container base and at the soil surface in the free-field during the moderate Port Island event in experiments T3-30, T3-50-SILT, and T3-50.

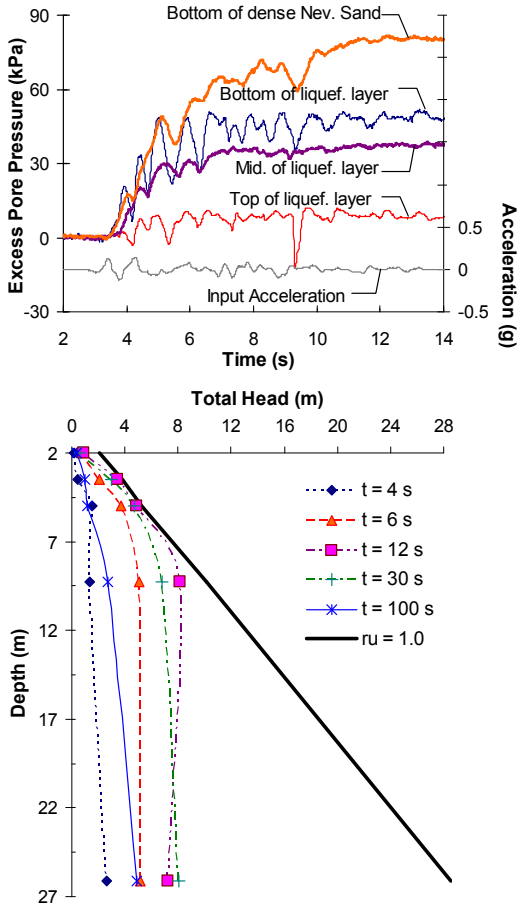

Fig. 11. Representative excess pore water pressure-time histories and total head isochrones in the free-field during the moderate Port Island event in T3-50.

Free-field settlements were initially quite similar during all three experiments (Fig. 12). The re-stiffening of the silt layer in T3-50-SILT after strong shaking likely led to the slowing of free-field surface settlements and caused long-term heave due to water flowing from under the buildings toward the free-field (Dashti et al. 2010a). Settlements continued at a higher rate in experiment T3-50 (with no silt layer) throughout shaking, but slowed down more rapidly compared to those measured during T3-30. The greater tendency for horizontal flow towards the free-field in T3-30 continued to supply excess pore water pressures that dissipated upward vertically. As a result, volumetric straining in the free-field continued for a longer period of time by extending the duration and intensity of soil particle disturbance and liquefaction and by supplying the vertical hydraulic gradients that control the rate of flow and volumetric strains.

Displacement measurements were made at different depths in the free-field in experiment T3-50 to understand better the settlement response within different soil layers. Fig. 13 shows

the settlement-time histories recorded at various depths in the free-field along with the corresponding volumetric strains within each soil layer in experiment T3-50 during the moderate Port Island event. It appears that the settlements observed in the free-field during the early parts of shaking were mostly due to settlements within the lower layer of Nevada Sand. As shown in Fig. 13, this "dense" layer was responsible for up to 60% of the total free-field settlements measured on the soil surface due to its large thickness, although it experienced negligible volumetric strains (as expected due to its high relative density). This settlement was likely primarily caused by the vertical upward flow that started soon after shaking. It is also likely that the upper parts of this dense layer experienced large sedimentation-induced volumetric strains ($\varepsilon_{p\text{-}SED}$) due to excessive strength loss (shown in Fig. 11).

The upward flow away from the lower dense layer toward the liquefiable deposit appeared to have delayed settlements within the upper layers. Following the initial settlements within the lower dense layer, large settlements were measured within the liquefiable deposit (primarily within its lower half). This layer went through large sedimentation- and consolidation-induced volumetric settlements ($\varepsilon_{p\text{-}SED}$ and $\varepsilon_{p\text{-}CON}$), while its response was likely strongly affected by the in-flow of water from the lower sand deposit and out-flow of water toward the surface during and after shaking.

SETTLEMENT OF BUILDINGS

Representative excess pore water pressure- and settlement-time histories recorded under the baseline structure A during the moderate Port Island event in experiments T3-30, T3-50-SILT, and T3-50 are shown in Fig. 14. The input base acceleration time-history recorded during T3-50 is also shown. Structures began to settle after one significant loading cycle. Buildings settled significantly more during T3-30 compared to the other two experiments. Building settlement rates reduced dramatically and almost stopped after the end of strong shaking (t ≈ 10-12 s) in T3-50-SILT and T3-50 while they continued at a rapidly decreasing rate in T3-30 beyond the end of strong shaking. More significant excess pore water pressure generation and strength loss under structures within the looser soil in T3-30 (D_r = 30%) amplified key liquefaction-induced displacement mechanisms during and after strong shaking. In addition to the higher resistance to pore water pressure generation and the smaller void space available for volumetric densification, the greater stiffness and dilative tendency of the D_r = 50% sand likely arrested shear strains under buildings sooner. These observations may not apply to buildings with larger height/width (H/B) ratios and larger building inertial loads, because they may respond more vigorously to amplified ground oscillations resulting from an increase in the soil's relative density. In fact, as shown in Fig. 15, Structure C (with the largest H/B ratio and contact pressure) settled more in T3-50-SILT than in T3-30 during the large Port Island motion likely due to amplified SSI-induced building ratcheting into the softened ground ($\varepsilon_{q\text{-}SSI}$).

The average building vertical displacement-time histories in T6-30, T3-30, and T3-50-SILT during the more intense, large Port Island event are shown in Fig. 15. Average free-field displacement-time histories as well as the input ground motion (during T3-30) are also provided for comparison. Structures settled in a similar manner as the moderate Port Island event (Fig. 14). Building settlement rates reduced dramatically after the end of strong shaking (t ≈ 12 s) and became negligible at the end of shaking (t ≈ 25 s). The observed trends during the moderate and large Port Island events suggest that the contribution of post-shaking reconsolidation settlements to the total building settlement must have been relatively minor in these experiments. As a result, other volumetric and deviatoric mechanisms of settlement must have been responsible for the majority of building settlements that occurred during shaking. The link between the initiation and intensity of shaking and the initiation and rate of building settlements, respectively, highlights the importance of cyclic inertial forces acting on the structure. Additionally, the effects of partial drainage during earthquake shaking on the responses of the soil and structure are important during these experiments.

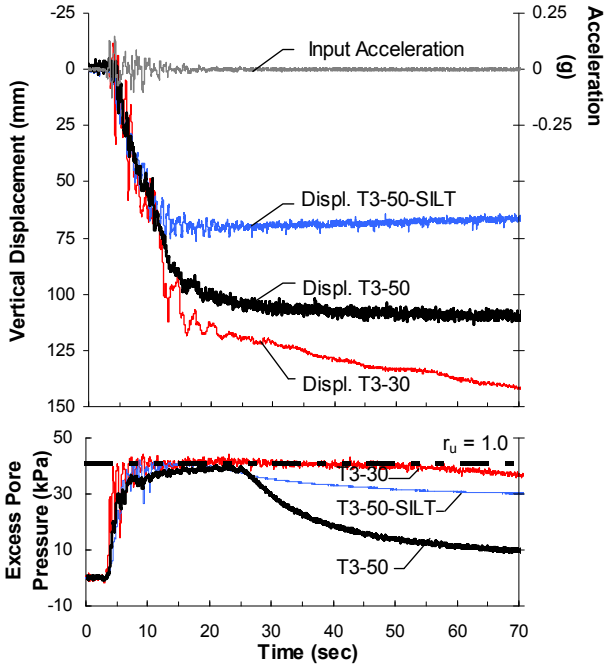

Fig. 12. Excess pore water pressure-time histories at the mid-depth of the looser layer of Nevada sand and soil surface settlements recorded in the free-field during the moderate Port Island event in experiments T3-30, T3-50-SILT, and T3-50.

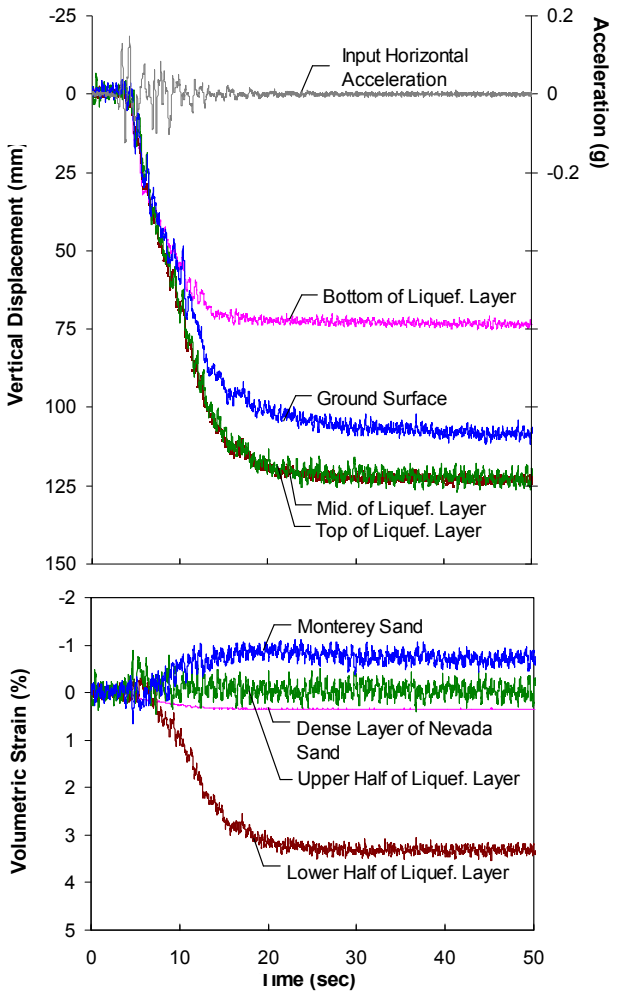

Fig. 13. Settlement-time histories at various depths along with the corresponding volumetric strains within each soil layer in the free-field during the moderate P.I. event in T3-50.

Fig. 16 compares representative transient hydraulic gradients that formed around Structure B in experiment T3-30 within the liquefiable layer during the large Port Island motion. In this experiment, large hydraulic gradients formed vertically upward and horizontally away from the building foundations within the liquefiable layer after a few seconds of strong shaking. Excess pore water pressures maintained their peaks throughout strong shaking while oscillating vigorously. After the end of strong shaking, a rapid reduction in excess pore water pressures underneath the structures was observed for approximately 20 seconds. This response was expected, as no significant excess pore water pressures were being generated during this time and the 3-D hydraulic gradients were near their peak values. After both vertical and horizontal hydraulic gradients declined, slower upward vertical pore water pressure dissipation began to control the flow under buildings until pore water pressures approached the hydrostatic condition.

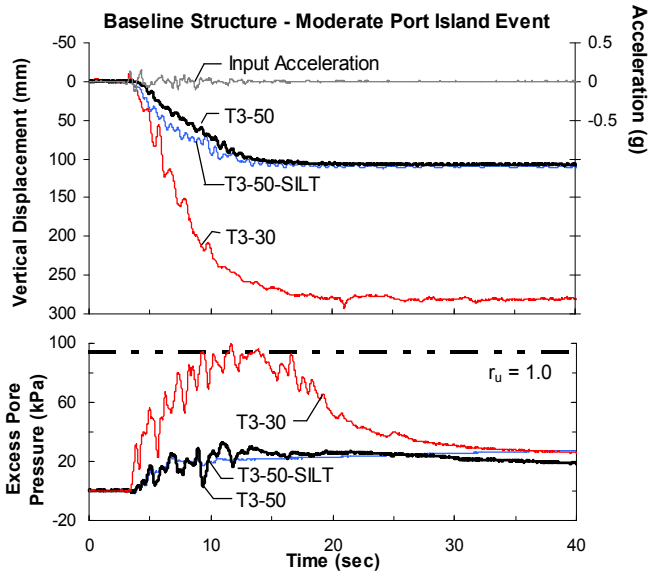

Fig. 14. Excess pore water pressure recordings at the mid-depth of the liquefiable layer under the baseline and average building vertical displacement-time histories in experiments T3-30, T3-50-SILT, and T3-50 during the moderate P.I. event.

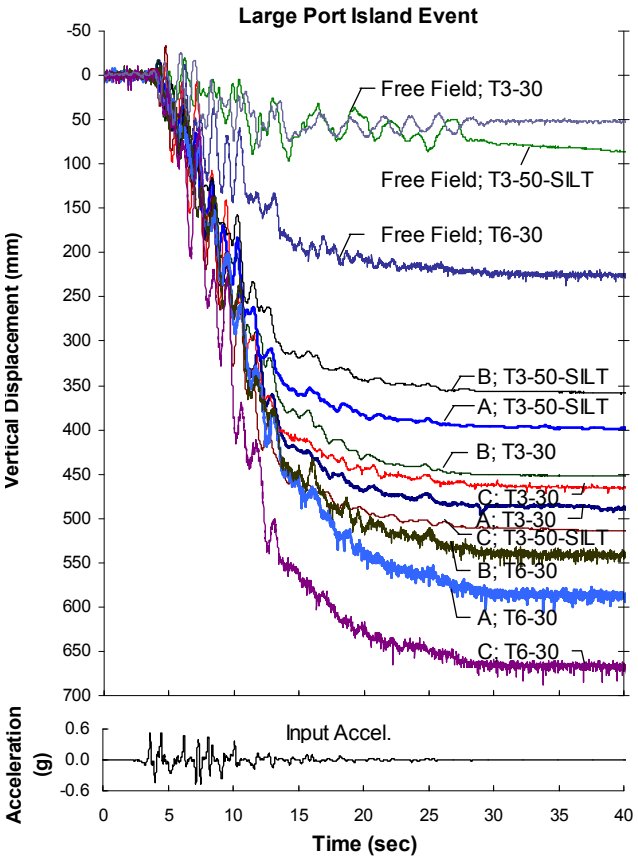

Fig. 15. Settlement-time histories in experiments T6-30, T3-30, and T3-50-SILT during the large P.I. event.

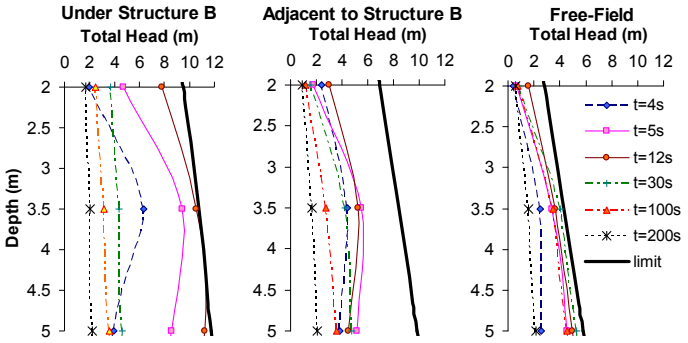

Fig. 16. Representative total head isochrones measured under and adjacent to a structure and in the free-field in experiment T3-30 during the large P.I. event (zoomed into the thickness of the liquefiable layer).

Previous physical model studies indicated primarily that water flowed laterally away from the liquefiable soil beneath the foundations. Liquefaction ($u_e \cong \sigma'_{vo}$) was not observed underneath the buildings in most cases and smaller excess pore water pressure ratios ($r_u = u_e / \sigma'_{vo}$) were created under the structural models compared to the free-field. Liu and Dobry (1997) attributed this effect to the dilative response of sand under initial static shear stresses imposed by the structure ($\alpha = \tau_{static}/\sigma_{vo}' > 0$). Sand under higher confinement and under the initial static shear stresses imposed by the structure is more resistant to pore water pressure generation than sand in the free-field. However, sand under higher confinement is capable of sustaining larger net excess pore water pressures (for the same r_u value) if subjected to sufficiently strong ground motions. As was shown in the Dashti (2009) study, net excess pore water pressures generated under the structure appear to be a function of the properties of the structure (e.g., weight, contact area, and height of the center of gravity), liquefiable soil (e.g., thickness and relative density), and the ground motion. The direction of flow was primarily away from underneath the foundations in experiment T3-30 during all shaking events and in experiments T3-50-SILT and T3-50 during the large Port Island ground motion. This indicates that higher excess pore water pressures were generated within the liquefiable soil under the buildings during these events. Water did flow laterally towards the liquefiable soil underneath the foundations in some other shaking events in experiments T3-50-SILT and T3-50.

During the large Port Island event, in contrast to the displacement patterns observed in the free-field, approximately 96±2% of total building settlements in T6-30 and T3-30 occurred during shaking. Post-shaking structural settlements were completed within 50 to 70 seconds in these experiments, after which buildings essentially stopped moving. In experiment T3-50-SILT, however, the presence of the low-permeability silt layer on top of liquefiable Nevada Sand slightly increased the contribution of post-earthquake structural settlements. The structures achieved approximately 90±5% of their total permanent settlements during shaking in T3-50-SILT, and around 5±2% of their total displacements occurred 170 s after the end of shaking. In addition to slower volumetric settlements caused by slower flow, void redistribution within Nevada Sand that was capped by silica flour likely reduced the soil's resistance to static building loads for an extended time after shaking stopped. This likely led to additional post-earthquake building settlements during T3-50-SILT.

The normalized average permanent building settlements measured during the large Port Island event in the first three centrifuge model tests are shown in Fig. 17. Results from the available case histories and experiments are also included in this figure. The building settlements plotted in Fig. 17 were estimated as the total settlement of structures minus the average settlement of the lower deposit of dense Nevada Sand during the large Port Island motion. Settlements were then normalized by the initial thickness of the liquefying layer (H_L). The results of T6-30, where the liquefiable layer was relatively thick (i.e., H_L = 6 m), were consistent with the results from previous experiments and case histories involving deep deposits of liquefiable materials. The results of T3-30 and T3-50-SILT, where the liquefiable layer was relatively thin (i.e., H_L = 3 m), were not consistent with other experimental results and case history observations.

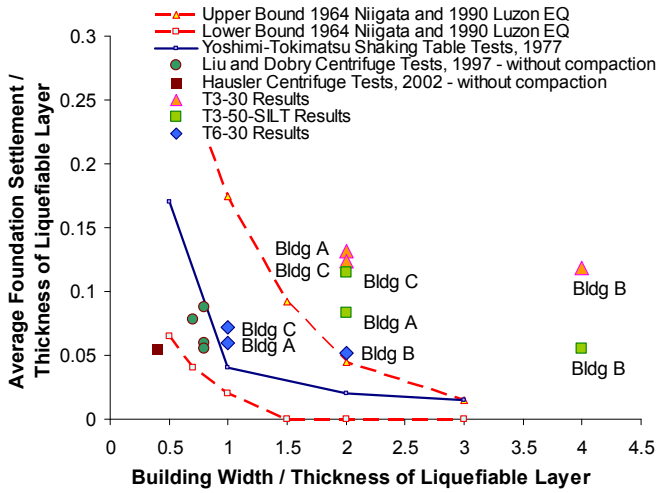

Fig. 17. A comparison of the normalized foundation settlements obtained from three centrifuge experiments during the large Port Island event with the available case histories and physical model tests (from Dashti et al. 2010a). This normalization does not work for the cases involving relatively thin layers of liquefiable soil (i.e., H_L = 3 m for the T3-30 and T3-50-SILT tests). Therefore, this type of normalization should not be used for these cases.

If there is a sufficient thickness of liquefiable soil present under building foundations, significant liquefaction-induced building settlements can occur that are not proportional to the thickness of the liquefying layer. Liquefaction-induced

building settlements in these cases are governed by deviatoric strains. Settlement is not governed by volumetric strains. Therefore, building settlement is not proportional to the thickness of the liquefiable layer as would be suggested if it were governed by volumetric strains. These results indicate that normalizing building settlement by the thickness of the liquefiable layer is misleading in understanding the response of different structures founded on relatively thin, shallow deposits of saturated granular soils. Therefore, this type of plot should not be used in engineering practice. The results also highlight the need for a better understanding of the primary factors influencing liquefaction-induced building settlements.

SEISMIC RESPONSE OF BUILDINGS

The settlement-time histories of the base-line structure A and soil surface in the free-field in experiment T3-50 during different earthquake scenarios are depicted in Fig. 18. Arias Intensity-time histories of the input motions are shown as well. Arias Intensity (I_a) is an index representing the energy of the ground motion in units of L/T (Arias 1970) and defined as

$$I_a(T) = \frac{\pi}{2 \cdot g} \int_0^T a^2(t) \cdot dt \qquad (1)$$

over the time period from 0 to T, where a = the measured acceleration value.

The TCU078 motion (see Table 1) was selected for its longer duration and slower rate of energy build-up compared to the Port Island motions. As shown in Fig. 18, the rate and duration of structural settlements observed during the TCU078 motion differed from those during the Port Island motion. Structures underwent smaller settlements, although they settled for a longer time period. Although the Arias Intensity and significant duration of the TCU078 event were respectively two and three times larger than those during the moderate Port Island event, structures settled less during the TCU078 earthquake. Therefore, even though a measure such as Arias Intensity describes many characteristics of a ground motion, it alone does not capture all of the potentially important effects of a ground motion on building settlement. Simpler ground motion measures, such as PGA and PGV, are even more deficient. Additional work is required to develop a more complete set of ground motion measures for this problem.

Structure A settled as much or more than the free-field soil surface in each experiment, except during the TCU078 motion in T3-50. Settlement of the lower dense deposit of Nevada Sand was negligible across the model during the TCU078 motion. The looser layer of Nevada Sand, however, developed large excess pore water pressures and experienced liquefaction in the free-field. Thus, relatively large volumetric strains were observed at locations away from the structures (i.e., in free-field) due to particle sedimentation ($\varepsilon_{p\text{-}SED}$), consolidation ($\varepsilon_{p\text{-}CON}$), and drainage ($\varepsilon_{p\text{-}DR}$) within the liquefiable layer. Smaller net excess pore pressures were measured within this layer under the buildings. These excess pore water pressures were too small to cause significant sedimentation, consolidation, volumetric strains due to localized drainage, or shear-type displacements due to partial bearing capacity failure under the buildings. As a result, structural settlements were mainly controlled by SSI-induced building ratcheting ($\varepsilon_{q\text{-}SSI}$). The settlement mechanisms activated under the buildings were not sufficient to overcome the greater volumetric-type settlements within the liquefiable layer in the free-field. This resulted in the structures settling less than the free-field soil surface during this earthquake. These observations confirm that the pore water pressure response at key locations and the triggering and magnitude of various settlement mechanisms are controlled by the interacting effects of soil relative density, structural properties, and the rate at which ground motion energy is built-up.

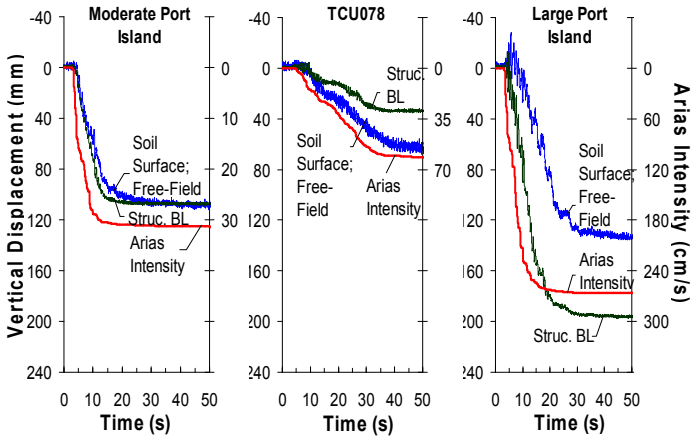

Fig. 18. Vertical displacement of the base-line structure and soil surface in the free-field in experiment T3-50 during different shaking events and the corresponding Arias Intensity time histories of the input motions.

The settlement-time history of the baseline building during each earthquake appeared to follow the shape of the Arias Intensity-time histories of each motion (Dashti et al. 2010b; e.g., see Fig. 18). The Arias Intensity of an earthquake motion depends on the intensity, frequency content, and duration of the ground motion. Its rate represents roughly the rate of earthquake energy build-up. This rate may be quantified by the Shaking Intensity Rate (*SIR*; Dashti et al. 2010b) as

$$SIR = I_{a5\text{-}75}/D_{5\text{-}75} \qquad (2)$$

where $I_{a5\text{-}75}$ is the change in Arias Intensity from 5% to 75% of its total value during which it is approximately linear in these tests, and $D_{5\text{-}75}$ is its corresponding time duration. The *SIR* of a ground motion represents the rate of soil particle disturbance, excess pore pressure generation, seismic demand on structures, and the resulting SSI effects in the foundation soil. As a result, the initiation, rate, and amount of

liquefaction-induced building settlement are expected to correlate to *SIR*. By combining the effects of ground motion intensity, frequency content, and duration, the parameter *SIR* better defines the seismic demand in terms of liquefaction-induced building settlement than the more conventionally used cyclic stress ratio (*CSR*).

The trends in the initial settlement rate of the baseline structure as a function of the shaking intensity rate (*SIR*) and the pre-event relative density (D_r) of the liquefiable soil are shown in Fig. 19. The results take into account the approximate change in the relative density of the liquefiable layer in each successive earthquake event. The level of shaking in these experiments is sufficient to induce liquefaction in the free-field. This chart does not include the influence of variations in the liquefiable layer thickness or structural properties. The results indicate that the rate of settlement increases as a motion's *SIR* increases and as the soil D_r decreases. The apparent dependency of building settlement on *SIR* may allow *SIR* to be used in combination with other parameters in procedures that evaluate the consequences of liquefaction.

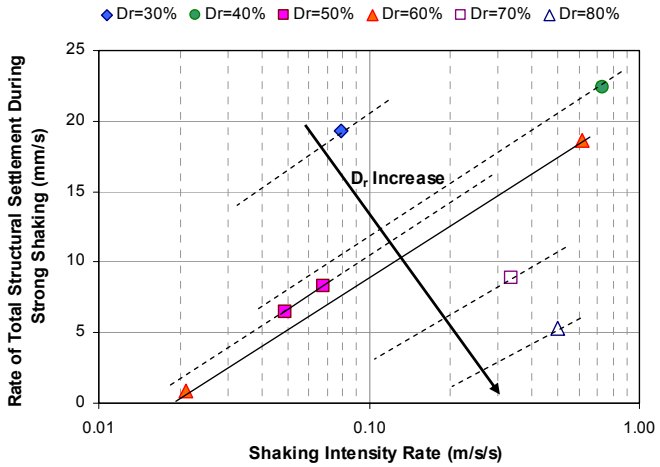

Fig. 19. Trends in the initial building settlement rate in experiments with a 3 m-thick liquefiable sand; SIR = $I_{a5\text{-}75}/D_{5\text{-}75}$ (from Dashti et al. 2010b).

INSIGHTS FROM NUMERICAL ANALYSES

Considerable effort has been devoted towards developing advanced numerical methods for performing nonlinear effectives stress analysis in which cyclic pore water pressure generation and the resulting seismic deformations are coupled. Numerous soil constitutive models and computational software have been developed for performing these types of analyses. For example, the UBCSAND1 constitutive model developed by Professor Peter Byrne at the University of British Columbia is a well-calibrated nonlinear effective stress model that is widely used by researchers and practicing engineers. It is commonly used in the computer code FLAC (Fast Lagrangian Analysis of Continua; Itasca 2008). Pore fluid stiffness and Darcy's flow rule are included in the FLAC program and drained, undrained, or coupled flow conditions can be specified by the user. The UBCSAND1 model has been used previously to guide the retrofit design of critical projects and has been shown to capture the trends observed in laboratory tests performed on clean sand (e.g., Puebla et al. 1997; Puebla 1999) as well as in centrifuge tests (Byrne et al. 2004).

Fully coupled nonlinear effectives stress analyses were performed using the UBCSAND1 model in the program FLAC-2D as part of this study to back-analyze the results obtained from the four well-documented centrifuge experiments performed by Dashti (2009), which were discussed previously. The goal was to evaluate the capabilities of the UBCSAND1 model to capture the primary observations made in these experiments and after doing so, investigate the seismic performance of different buildings founded on shallow layers of liquefiable sand of varying density and thickness.

The UBCSAND1 soil model was calibrated to capture the liquefaction triggering response in accordance with field observations (e.g., Idriss and Boulanger 2008). UBCSAND1 elastic and plastic parameters were adjusted so that the model would be in close agreement with field observation for each value of $N_{1,60}$ considered. The liquefaction response of Nevada Sand for the relative densities of interest (approximately 30-40%, 50%-60%, and 90%) was then more precisely calibrated based on the available cyclic simple shear tests that were carried out for the VELACS project by Arulmoli et al. (1992) and at the University of California at Berkeley by Kammerer et al. (2000).

In calibrating the elastic and plastic parameters and hydraulic conductivities for each soil layer, an iterative process was employed to capture reasonably the liquefaction triggering and the post-triggering responses observed in the field, in cyclic simple shear tests, and in the centrifuge experiment of interest. Fig. 20 presents the relationship between the model's estimate of the *CSR* to cause liquefaction in 15 cycles versus the sand's corrected SPT blow counts ($N_{1,60}$) with the relationship proposed by Idriss and Boulanger (2008) based on field observations. Fig. 21 compares the UBCSAND1 model's estimate of the liquefaction resistance of Nevada Sand with cyclic simple shear test data. For both the laboratory tests and the numerical analyses, liquefaction was assumed to trigger when the absolute value of single amplitude cyclic shear strains reached 3.75%. Fig. 22 provides a sample comparison of the predicted and measured response in a cyclic simple shear test on Nevada Sand with relative a density of about 50%. These comparisons show that UBCSAND1 can capture the build-up of excess pore water pressure, liquefaction triggering, and post-triggering strain accumulation reasonably well.

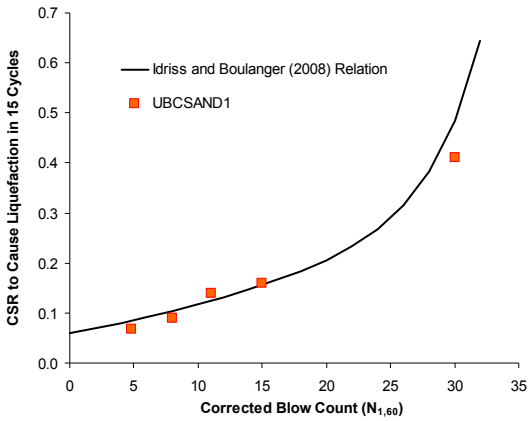

Fig. 20. Comparison of predicted and field-observed liquefaction triggering response

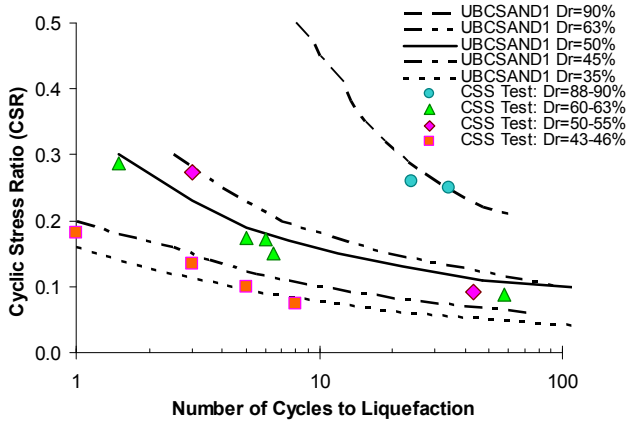

Fig. 21. Liquefaction resistance of Nevada Sand in cyclic simple shear tests and as estimated using UBCSAND1.

Values of hydraulic conductivity available for Nevada Sand were measured under 1 g field conditions. Slight variations in the gradation of the batch of Nevada Sand used can affect measured values significantly. Additionally, the soil's hydraulic conductivity has also been shown to increase as it liquefies (e.g., Jafarzadeh and Yanagisawa 1995), which further increases the potential for drainage during cyclic loading. Consequently, the value of each soil layer's vertical hydraulic conductivity was adjusted slightly to capture the pore pressure response measured in the free-field during the centrifuge experiments. Additionally, the lateral flow of water from underneath the 3-D structural models used in the centrifuge tests is not captured by these 2-D plane strain FLAC analyses. Thus, excessively large excess pore water pressures were calculated initially in the liquefiable sand underneath the building in these analyses. To reduce this error, the horizontal hydraulic conductivity of the looser layer of Nevada Sand was increased to allow for more horizontal flow near the structure. Table 2 summarizes the calibrated values of hydraulic conductivity used to model each soil layer.

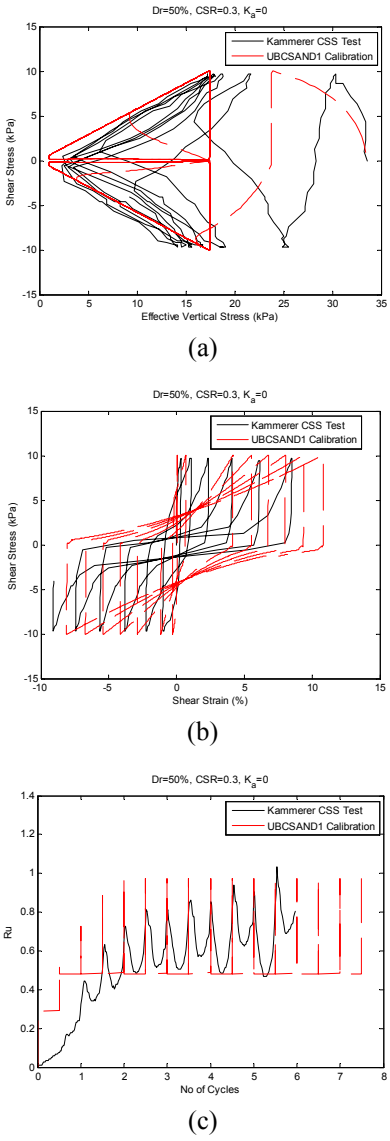

Fig. 22. A comparison of the UBCSAND1 predicted response with that measured in a cyclic simple shear test on Nevada Sand (D_r=50%, CSR=0.3, K_α=0): (a) stress path; (b) shear stress-shear strain relationship; and (c) excess pore water pressure ratio time-history.

Table 2. Values of sand hydraulic conductivity used in FLAC-2D numerical analyses

Soil Layer	Horizontal Hydraulic Conductivity (cm/s)	Vertical Hydraulic Conductivity (cm/s)
Dense Nevada Sand	5E-03	5E-03
Loose to Medium Dense Nevada Sand	2	5E-03
Monterey sand	7E-01	7E-01

The responses near and away from Structure A in the Dashti (2009) centrifuge experiments were simulated using FLAC-2D with the calibrated UBCSAND1 model. The finite difference model is shown in Fig. 23, and representative comparisons of the numerical and centrifuge test results during the moderate Port Island event in experiments T3-50 and T3-30 are shown in Figs. 24-28. Displacement estimates were generally more accurate near the structure than those in the free-field, because displacements near structures were dominated by shear-type mechanisms (Figs. 24 through 26). Settlements were largely under-predicted within liquefiable Nevada Sand in the free-field, where sedimentation-type volumetric settlements ($\varepsilon_{p\text{-}SED}$) were large (Fig. 24). Settlements due to sedimentation ($\varepsilon_{p\text{-}SED}$) are not captured by the soil models that are currently available.

Although these analyses did not capture accurately each individual settlement mechanism (e.g., $\varepsilon_{p\text{-}SED}$ and $\varepsilon_{p\text{-}DR}$), liquefaction-induced building settlements were predicted reasonably (Fig. 25), because the UBCSAND1 model captures the primary deviatoric displacement mechanisms well. Additionally, a fully-coupled numerical analysis with carefully calibrated values of hydraulic conductivity is expected to capture reasonably localized volumetric strains due to partial drainage during dynamic loading ($\varepsilon_{p\text{-}DR}$). These comparisons suggest that a fully coupled, effective stress analysis with the UBCSAND1 constitutive model is capable of capturing the primary mechanisms of building settlement for the conditions investigated in this study.

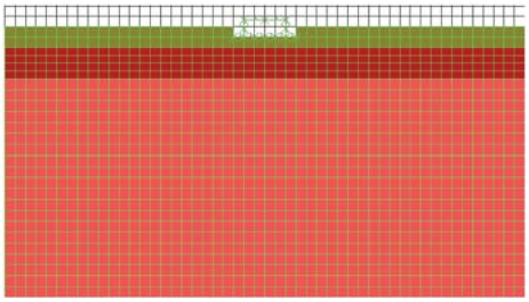

Fig. 23. The mesh configuration in FLAC-2D numerical analyses modeling experiment T3-50.

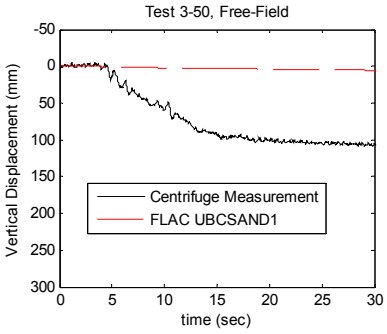

Fig. 24. A comparison of FLAC estimated free-field settlements with those recorded in experiment T3-50 during the moderate P.I. event.

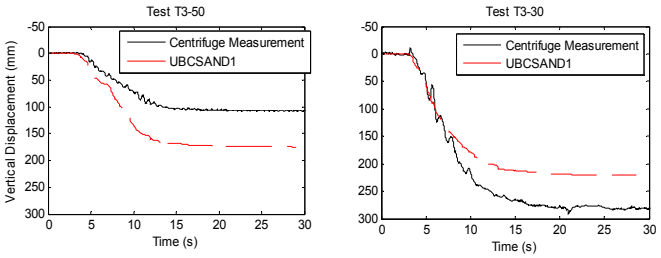

Fig. 25. A comparison of FLAC estimated settlements with those recorded under Structure A in experiments T3-50 and T3-30 during the moderate P.I. event.

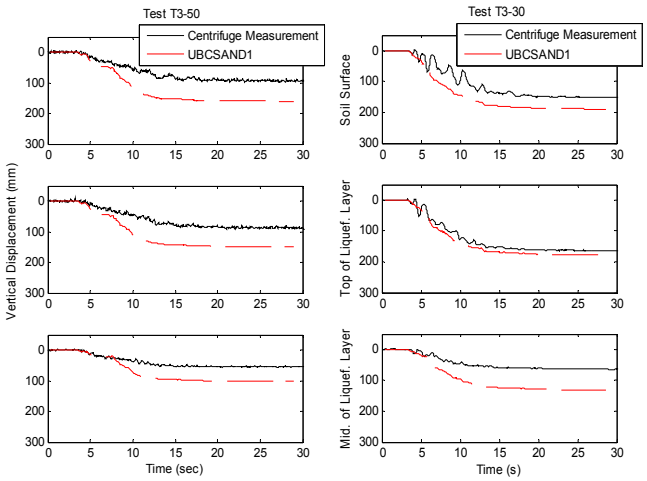

Fig. 26. A comparison of FLAC predicted soil settlements adjacent to Structure A with those recorded during experiments T3-50 and T3-30, moderate P.I. event.

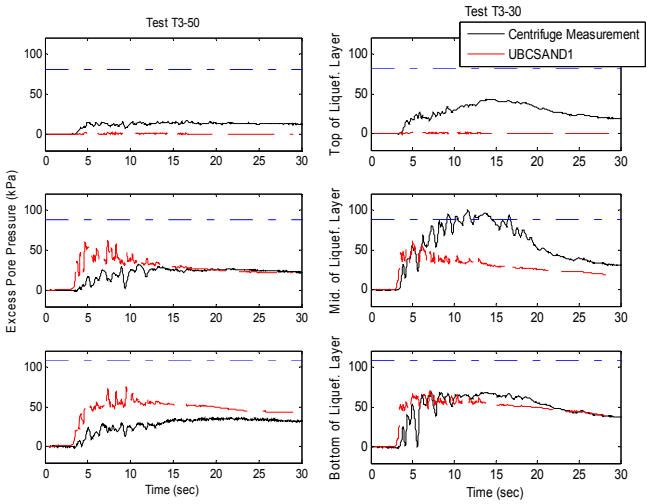

Fig. 27. A comparison of FLAC predicted excess pore water pressure-time histories under Structure A with those recorded during experiments T3-50 and T3-30, moderate P.I. event.

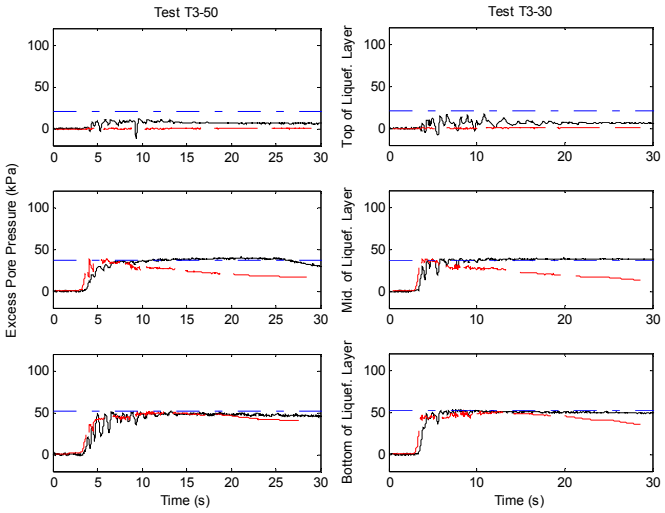

Fig. 28. A comparison of FLAC predicted excess pore water pressure-time histories in the free-field with those recorded during experiments T3-50 and T3-30, moderate P.I. event.

RECOMMENDATIONS FOR PRACTICE

The observations of ground and building performance in Adapazari, Turkey during the 1999 Kocaeli earthquake (as well as similar types of observations observed in Taiwan during the 1999 Chi-Chi earthquake), the results of the Dashti (2009) centrifuge tests, and the insights gained from the nonlinear effective stress analysis using the UBCSAND1 soil model provide guidance regarding how to evaluate liquefaction-induced building movements in engineering practice. As this is a complex problem and the numerical studies are ongoing, this guidance should be considered as being preliminary. Additional work on this important topic is required. The profession has largely addressed the liquefaction triggering evaluation problem. However, there is much work to be done to understand fully the consequences of liquefaction. Reliable procedures for estimating liquefaction-induced building movements can only be developed when the governing mechanisms are understood well.

Whereas both volumetric-induced and deviatoric-induced displacement mechanisms contribute to liquefaction-induced building movements during and after strong shaking, the governing mechanisms are primarily deviatoric-induced when the liquefiable soil layer is sufficiently thick and close to the building foundation. Methods that estimate free-field settlement (e.g., Tokimatsu and Seed 1987; Ishihara and Yoshimine 1992) cannot be used to estimate liquefaction-induced building settlements for this case (i.e., shallow foundation atop a shallow layer of liquefiable soil). These procedures were developed to estimate post-liquefaction reconsolidation ground settlements in the absence of buildings. They were developed and calibrated to capture only volumetric-induced reconsolidation strains. Thus, they cannot be used when deviatoric-induced displacement mechanisms are important, as is the case with liquefaction-induced building displacements.

It is inappropriate to normalize building settlements or the width of its foundation by the thickness of the soil layer that liquefied. This type of normalization implies that volumetric-induced displacement mechanisms govern building settlement. They do not when the liquefiable soil layer is shallow. Instead, deviatoric-induced displacement mechanisms govern the response of the building as the rocking heavy building repeatedly pushes itself into the liquefied soil that is sheared under this loading. Volumetric strain is also induced during this cyclic loading of the soil, but it is the SSI-induced foundation ratcheting deformations ($\varepsilon_{q\text{-}SSI}$) and partial bearing failure due to soil strength loss deformations ($\varepsilon_{q\text{-}BC}$) that govern primarily building movements. Localized volumetric strains resulting from partial drainage in response to intense transient hydraulic gradients ($\varepsilon_{p\text{-}DR}$) are important, but in many cases, settlement due to sedimentation after liquefaction ($\varepsilon_{p\text{-}SED}$) and consolidation ($\varepsilon_{p\text{-}CON}$) are less important.

If liquefaction is triggered in the free-field, it is likely that liquefaction will occur under the edges of a building's shallow foundation and in the soil adjacent to the foundation. In fact, numerical studies by Travasarou et al. (2006) found that the factor of safety for liquefaction triggering was significantly underestimated using the free-field condition because shallow soils adjacent to the building are subjected to higher cyclic shear stresses due to the rocking and horizontal shaking of the building and higher cyclic stress ratios because of the absence of the building's static pressure. The combined effect is a reduced factor of safety against liquefaction, which can be as much as 50% of the corresponding free-field value. Thus, it is appropriate to increase the seismic demand around the perimeter of structures when performing liquefaction triggering evaluation for buildings where potentially liquefiable layers are located at shallow depths or immediately underneath the foundation. This is particularly important for the case of marginally liquefiable layers, when the results of a free-field liquefaction triggering evaluation may be misleading.

If significant pore pressures are generated in shallow soil deposits that are underneath and adjacent to the edges of a shallow building foundation, the engineer should evaluate liquefaction-induced building movements. At this time, no reliable simplified procedure is available to assist in this evaluation. A well-calibrated nonlinear effective stress dynamic analysis can be performed to provide insight, and this should be done for projects when it is important to develop reliable estimates of building movement. These relatively sophisticated analyses should only be performed by well trained and experienced engineers with a calibrated model.

At this time, it may be infeasible economically to perform nonlinear effective stress analysis for many other projects. Ground improvement or seismic retrofitting should be considered as they can be used to eliminate or minimize the

problems associated with liquefaction-induced building movements. In developing the mitigation measures, the primary governing mechanisms should be considered. A mitigation measure that does not arrest the primary displacement mechanisms, which are likely deviatoric-induced displacement mechanisms ($\varepsilon_{q\text{-}SSI}$ and $\varepsilon_{q\text{-}BC}$) and localized volumetric strains resulting from partial drainage ($\varepsilon_{p\text{-}DR}$), will not achieve the desired seismic performance.

The seismic bearing capacity of a building founded on shallow liquefiable soils should be evaluated first with a procedure that considers the dynamic inertial loading of the building. Most importantly, the analysis should be performed using the post-liquefaction residual shear strength of the liquefied soil. If the dynamic factor of safety using post-liquefaction residual strength approaches one, then a global instability and toppling are possible. For cases in which the factor of safety approaches 1.5, large differential building settlements are still possible.

In cases that pass this instability screening analysis in which the liquefaction-induced building displacements are to be evaluated in an approximate manner, volumetric-induced strains can be estimated using conventional approaches such as Ishihara and Yoshimine (1992) or Zhang et al. (2002). The volumetric-induced settlement estimated with this type of approach must be combined with that resulting from deviatoric-induced movements. Deviatoric-induced settlement can be roughly estimated using the concept of liquefaction-induced shear strain potential (e.g., Shamoto et al. 1998, Zhang et al. 2004, Idriss and Boulanger 2008, and Cetin et al. 2009).

Considerable judgment is required, because intense, localized deviatoric strains and volumetric strains can accumulate to produce large building settlements. Special attention should be given to taller buildings with high aspect ratios (i.e., $H/B > 1.5$), which are more prone to tilting or extreme differential settlements. SSI-ratcheting induces significant settlement in taller/heavier structures. The amount of vertical displacement of the building relative to the surrounding ground is roughly proportional to the aspect ratio of the building (i.e., H/B), which is relatively equivalent to the applied contact pressure. All else being equal, buildings of higher contact pressure (and also higher aspect ratio) experience more vertical displacement. Regardless of the width of the foundation, on average, taller/heavier buildings experience greater vertical movement than smaller/lighter buildings.

CONCLUSIONS

Seismically induced settlement of buildings with shallow foundations on liquefiable soils has resulted in significant damage in recent earthquakes. For example, multi-story buildings punched into, tilted excessively, and slid laterally on softened ground in Adapazari, Turkey. Recent geotechnical centrifuge experiments coupled with dynamic analyses provide useful insights.

The geotechnical centrifuge tests performed by Dashti (2009) revealed that considerable building settlement occurs during earthquake strong shaking. Volumetric strains due to localized drainage in response to high transient hydraulic gradients and deviatoric strains due to shaking-induced ratcheting of the buildings into the softened soil are important effects that are currently not captured in current procedures. The relative importance of each mechanism depends on the characteristics of the earthquake motion, liquefiable soil, and building. The initiation, rate, and amount of liquefaction-induced building settlement depend greatly on the shaking intensity rate (*SIR*) of the ground motion.

The dominant liquefaction-induced building displacement mechanisms for many cases involving shallow foundations on shallow deposits of liquefied soil were found to be SSI-induced foundation ratcheting deformations ($\varepsilon_{q\text{-}SSI}$), partial bearing failure due to soil strength loss deformations ($\varepsilon_{q\text{-}BC}$), and localized volumetric strains resulting from partial drainage in response to intense transient hydraulic gradients ($\varepsilon_{p\text{-}DR}$). If excess pore pressures reached the initial effective vertical stress during earthquake shaking (i.e., $r_u = u_e / \sigma'_{vo} \cong 1$), then sedimentation after liquefaction ($\varepsilon_{p\text{-}SED}$) also contributed significantly to the observed building settlement. In most cases, the contribution of consolidation-induced volumetric strains ($\varepsilon_{p\text{-}CON}$) to the total building settlement was relatively minor.

The state-of-the-practice still largely involves estimating building settlement using empirical procedures developed to calculate post-liquefaction consolidation settlement in the free-field. This approach cannot possibly capture shear-induced and localized volumetric-induced deformations in the soil underneath shallow foundations. Thus, other procedures should be used. Currently, simplified procedures that directly address this problem are not available. Recommendations are provided in this paper in the interim, but many of these recommendations are statements of what should not be done. The use of well-calibrated nonlinear effective stress analysis appears to be the most reliable path forward at this time other than eliminating the problem through ground improvement or foundation retrofitting. Significant additional work is required to advance the profession's understanding of this problem and to develop robust analytical procedures that can be used in engineering practice.

ACKNOWLEDGMENTS

This material is based in part upon work supported by the National Science Foundation (NSF) under Grant No. CMMI-0530714. Any opinions, findings, and conclusions or recommendations expressed in this material are those of the authors and do not necessarily reflect the views of the NSF. Drs. Juan Pestana and Michael Riemer of UC Berkeley and Dr. Daniel Wilson of UC Davis participated in the NSF-funded centrifuge testing program. Dr. Bruce Kutter of UC Davis shared insights. Centrifuge tests were performed at the

large geotechnical centrifuge at UC Davis, which is supported by the NSF George E. Brown, Jr. Network for Earthquake Engineering Simulation (NEES) program under Award No. CMMI-0402490. The staff at UC Davis was of great help in performing these tests. Dr. Rodolfo Sancio of Geosyntec Consultants, Inc. and Dr. Thaleia Travasarou of Fugro-West, Inc. participated in the field studies and original SSI analyses of buildings in Adapazari. Professor Peter Bryne of the Univ. of British Columbia shared his UBCSAND1 model with us and provided guidance on its use.

REFERENCES

Adalier, K., and Elgamal, A. [2005]. "Liquefaction of over-consolidated sand: a centrifuge investigation," *J. Earthquake Engineering*, 9(1), 127–150.

Arias, A. [1970]. "A measure of earthquake intensity." *Seismic design for nuclear power plants*, R. J. Hansen, ed., MIT Press, Cambridge, Mass.

Arulmoli, K., Muraleetharan, K.K., Hossain, M.M., Fruth, L.S. [1992]. "VELACS: Verification of Liquefaction Analyses by Centrifuge Studies, Laboratory Testing Program." Soil Data Report. Project No. 90-0562. The Earth Technology Corporation, Irvine, CA.

Bray, J.D., and Stewart, J. P. [2000]. "Damage Patterns and Foundation Performance in Adapazari," Chapter 8 of the Kocaeli, Turkey Earthquake of August 17, 1999 Reconnaissance Report, in *Earthquake Spectra J*., EERI, 16 (A), 163-189.

Bray, J. D., R. B. Sancio, H.T. Travasarou, T., Durgunoglu, A. Onalp, T. L. Youd, J. P. Stewart, R. B. Seed, O.K. Cetin, E. Bol, M. B. Baturay, C. Christensen, and T. Karadayilar, [2004]. "Subsurface Characterization at Ground Failure Sites in Adapazari, Turkey," *J. Geotech. Engng.*, ASCE, 130(7), 673-685.

Bray, J.D. and Sancio, R.B. [2006]. "Assessment of the Liquefaction Susceptibility of Fine-Grained Soils," *J. Geotech. Engng.*, ASCE, 132(9),1165-1177.

Byrne, P. M., Park, S. S., Beaty, M., Sharp, M., Gonzalez, and L., Abdoun, T. [2004]. "Numerical modeling of liquefaction and comparison with centrifuge tests," *Canadian Geotech. J.*, 41, 193-211.

Cetin, K.O., Bilge, H.T., Wu, J., Kammerer, A.M., and Seed, R.B. [2009]. "Probabilistic models for cyclic straining of saturated sand," *J. Geotech. Geoenviron. Engng*., ASCE, 135(3), 371-386.

Dashti, S. [2009]. "Toward evaluating building performance on softened ground," *Ph.D. Dissertation*, Univ. of Calif., Berkeley.

Dashti, S., Bray, J.D., Pestana, J.M., Riemer, M.R. and Wilson, D. [2010a]. "Mechanisms of seismically-induced settlement of buildings with shallow foundations on liquefiable soil," *J. Geotech. Geoenviron. Engng*., ASCE, 136(1).

Dashti, S., Bray, J.D., Pestana, J.M., Riemer, M.R. and Wilson, D. [2010b]. "Centrifuge Testing to Evaluate and Mitigate Liquefaction-Induced Building Settlement Mechanisms," *J. Geotech. Geoenviron. Engng*., ASCE, in press.

Dobry, R., and Liu, L. (1992). "Centrifuge modeling of soil liquefaction," *Proc., 10th World Conference on Earthquake Engineering*, Int. Assoc. for Earthquake Engineering (IAEE), Madrid, Spain, 7801-6809.

Elgamal, A. W., Dobry, R., and Adalier, K. [1989]. ''Small scale shaking table tests of saturated layered sand-silt deposits,'' *2nd U.S.-Japan Workshop on Soil Liquefaction*, Buffalo, NY, NCEER Rep. No. 89-0032, 233–245.

Fiegel, G.L., and Kutter, B.L. [1994]. "Liquefaction-induced lateral spreading of mildly sloping ground," *J. Geotech. Eng.*, ASCE, 120(12), 2236-2243.

Hausler, E.A. [2002]. "Influence of ground improvement on settlement and liquefaction: a study based on field case history evidence and dynamic geotechnical centrifuge tests." *Ph.D. Dissertation*, Univ. of Calif., Berkeley, Ch. 5: 85-271.

Idriss, I.M, and Boulanger, R.S [2008]. "Soil liquefaction during earthquakes," EERI MNO-12, Oakland, CA.

Ishihara, K., and Yoshimine, M. [1992]. "Evaluation of settlements in sand deposits following liquefaction during earthquakes," *J. Soils and Foundations*, 32(1), 173-188.

Ishii, Y. and Tokimatsu, K. [1988]. "Simplified procedures for the evaluation of settlements of structures during earthquakes," *Proceedings from the Ninth World Conference on Earthquake Engineering*, Tokyo-Kyoto, Japan, 3, 95-100.

Itasca. FLAC, version 6.0. 2008, Itasca Consulting Group Inc., Minneapolis.

Jafarzadeh F. and Yanagisawa E. [1995]. "Settlement of sand models under unidirectional shaking." *Proc., 1st Int. Conf. on Earthquake Geotech*. Eng., K. Ishihara Ed., IS-Tokyo, Japan, Vol. 2, 693–698.

Kammerer, A., Wu, J., Pestana, J., Riemer, M., and Seed, R. [2000]. Cyclic simple shear testing of Nevada sand for PEER Center, project 2051999. *Geotechnical Engineering Research Report*, UCB/GT/00-01, University of California, Berkeley, Calif.

Kokusho, T. [1999]. "Water film in liquefied sand and its effect on lateral spread," *J. of Geotech. and Geoenviron. Engrg.*, ASCE, 125(10), 817-826.

Kulasingam, R., Malvick, E.J., Boulanger, R.W., Kutter, B.L. [2004]. "Strength Loss and Localization at Silt Interlayers in Slopes of Liquefied Sand." *J. Geotech. Geoenviron. Eng*., 130(11), 1192-1202.

Liu, H. [1995]. "An empirical formula for evaluation of buildings settlements due to Earthquake liquefaction," *Proc. 3rd Inter. Conf. Rec. Adv. Geotech. EQ Engrg. & Soil Dy*n., Vol. 1, pp. 289-293.

Liu, L. and Dobry, R. [1997]. "Seismic response of shallow foundation on liquefiable sand," *J. Geotech. Geoenviron. Engng.*, ASCE, 123(6), 557-567.

Meyerhof, G.G. [1964]. "Shallow foundations," *Proc. of the ASCE Conference on Design of Foundations for Control of Settlements*, Northwestern University, Evanston, IL, June.

Puebla, H., Byrne, P. M., and Philips, R. [1997]. "Analysis of CANLEX liquefaction embankments: prototype and centrifuge models," *Canadian Geotechnical Journal*, 34(5), 641-657.

Puebla, H. [1999]. "A constitutive model for sand and the analyses of the CANLEX Embankments," *Ph.D. Dissertation*, University of British Columbia, Canada.

Sancio, R. B., J. D. Bray, J. P. Stewart, T. L. Youd, H.T. Durgunoglu, A. Onalp, R. B. Seed, C. Christensen, M. B. Baturay, and T. Karadayilar [2002]. "Correlation Between Ground Failure And Soil Conditions in Adapazari, Turkey," *Soil Dyn. & EQ Engineering* J., 22 (9-12), 1093 - 1102.

Sancio, R., Bray, J.D., Durgunoglu, T., and Onalp, A, [2004]. "Performance of buildings over liquefiable ground in Adapazari, Turkey," *Proc., 13th World Conf. on Earthquake Engineering*, Vancouver, Canada, Paper No. 935.

Shahien, M.M. [1998]. "Settlement of Structures on Granular Soils Subjected to Static and Earthquake Loads," *Ph.D. Thesis*, Univ. of Illinois at Urbana-Champaign, Urbana, IL.

Shamoto, Y., Zhang, J.-M., and Tokimatsu, K. [1998]. "Methods for evaluating residual post-liquefaction ground settlement and horizontal displacement," *Soils and Foundations*, Spec. Issue on Geotech. Aspects of Jan. 17, 1995 Hyogoken-Nambu EQ, No. 2, Sept., 69-83.

Stewart, D.P., Chen, Y.R., and Kutter, B.L. [1998]. "Experience with the use of methylcellulose as a viscous pore fluid in centrifuge models," *Geotechnical Testing Journal*, ASTM, 21(4), 365-369.

Tokimatsu K., and Seed H.B. [1987]. "Evaluation of settlements in sands due to earthquake shaking," *J. Geotech. Engng.*, ASCE, 113(8), 861-878.

Travasarou, T., Bray, J.D., and Sancio, R.B. [2006]. "Soil-Structure Interaction Analyses of Building Responses During the 1999 Kocaeli Earthquake," *Proc. 8th US Nat. Conf. EQ Engrg.*, 100th Anniv. EQ Conf. Comm. the 1906 San Francisco Earthquake, EERI, April, Paper 1877.

Yoshimi, Y. and Tokimatsu, K. [1977]. "Settlement of buildings on saturated sand during earthquakes," *Soils and Foundations*, Vol. 17, No. 1, pp. 23-38.

Zhang, G., Robertson, P.K., and Brachman, R.W.I. [2002]. "Estimating liquefaction-induced ground settlements from CPT for level ground," *Canadian Geotechnical Journal*, 39, 1168-1180.

Zhang, G., Robertson, P.K., and Brachman, R.W.I. [2004]. "Estimating liquefaction-induced lateral displacements using the standard penetration test or cone penetration test," *J. Geotech. Engng.*, ASCE, 130(8), 861-871.